Empirical comparison of Chirp and Multitones on experimental UWB Software Defined Radar prototype

J. Le Kernec[1], O. Romain[2], P. Garda[3], J. Denoulet[3]
[1] University of Nottingham Ningbo, Ningbo, China
[2] Laboratoire ETIS UMR8051, Université Cergy Pontoise, France
[3] Laboratoire d'Informatique de Paris 6 - LIP6, UPMC, Paris, France
julien.lekernec@nottingham.edu.cn, olivier.romain@u-cergy.fr

***Abstract*—This paper proposes and tests an approach for an unbiased study of radar waveforms' performances. Using the ultrawide band software defined radar prototype, the performances of Chirp and Multitones are compared in range profile and detection range. The architecture was implemented and has performances comparable to the state of the art in software defined radar prototypes. The experimental results are consistent with the simulations.**

Keyword: Radar, Multitones, OFDM, UWB, Software Radio

I. INTRODUCTION

In the past decade, digital architectures gradually replaced analog circuitry. As a result, purely digital waveforms have emerged (Multitones being a prominent example that has a wide array of commercial applications). These purely digital waveforms allow increased data throughput and are more robust against fading having its primary commercial application in modern telecommunication standards such as wireless LAN [1]. To date, Multitones have seldom been used in radar applications.

The most common radar signal used is the linear frequency modulated pulse (also known as Chirp). This signal has been commonly used in radar for several decades [2]. The adoption of Multitones in radar applications hasbeen slow to develop for a variety of reasons. Commercial applications are unlikely to be developed unless and until there is a viable need for them. Recently, the use of a swarm of drones for reconnaissance missions are required to perform Synthetic Aperture Radar (SAR) imaging and networking simultaneously to maintain formation, and send/receive data while imaging the scene. This is not possible with just Chirp. As a result, there has been an increasing interest for the use of multifunction signals such as Multitones.

Recent advances in AD/DA converters and processing capabilities, synthesizing, digitizing and processing ultrawide band (UWB) signals is now feasible on a digital platform. This allows finer resolution for imaging applications, spectrum insertion and the use of signal and frequency agility. These advances also enable software defined radar, which can dynamically reconfigure its RF frontend, middleware and processing algorithms. Software defined radar can thus be multifunction switching from one mode to the other such as surveillance, tracking, imaging and also telecommunications.

The widespread adoption of Multitones will only be possible when the capabilities of the signal match the specific tasks that are required. Then and only then can Multitones be successfully integrated into applications and subsequently put to operational use. As such, it is the confluence of factors that ultimately determine the relevance and ultimate integration of Multitones for multifunction radar applications Specifically, developing a technology without first having a commercially viable application is unlikely.

Multitones are therefore seen as a good candidate for the next generation of digital radar. Multitones are phase-coded to reduce Peak-to-Mean Envelope Power Ratio (PMEPR) and improve power amplifier efficiency. The sub-band independence [3] allows an independent processing of each band for multifunction operation and ensures detection even in presence of frequency selective fading [4]. The signal diversity is important in terms of low probability of interception to evade radar counter measures and allow frequency reuse when multiple radars operate in the same vicinity [5]. As a result, our research question is how do Multitones signals compare to Chirp signals in multifunction radar applications?

The rest of the paper is developed as follows, section II reviews the literature on Multitones performances for radar applications and existing software defined radar platforms. Section III describes two possible radar architectures and the design considerations that lead to the chosen architecture for prototyping presented in section IV. Finally, in Section V, the radar waveforms' performances are compared in simulation and experimentally tested on the prototype.

II. LITERATURE REVIEW

There has been recent work dealing with the communication aspect of Multitones in radar without consideration of the performance of the radar [c.f. 6]. However, a few studies have examined the relative performance of Multitones in radar applications [7][8][9]. One such study [7] provided a simulation of single carrier and Multitones radar systems. They found that the required

constant false alarm rate detection threshold is lower for Multitones than for a single carrier radar system with polyphase codes. In short, they found a higher level of precision resulting from the use of Multitones.

Two additional studies have examined the relative performance of trains of diverse Multitone pulses coded in phase and amplitude [2][8]. Using this technique, they both achieve near thumbtack ambiguity functions. This ambiguity function does not suffer from range-Doppler coupling as does Chirp [2]. In both cases, this ambiguity function comes at the cost of a higher pedestal level. New processing capabilities are emerging such as Doppler resolution while using agility [8]. This particular feature cannot be performed with classic radar waveforms while using agility. In [9], the Doppler ambiguity is resolved over one pulse train.

Multitones show potential for new radar advances, such as Doppler resolution using agility [8]. However, it is important to note that the results for this part were mostly simulated results. It also appears that the basic performances of Multitones for radar systems are not well known and the literature lacks a viable reference to compare it to. Hence the simulations presented in section IV will be compared to experimental results described in part III. The reference in radar waveforms is the linear frequency modulated (LFM) [2] and its performances will be compared against Multitones' performances.

Concerning software radar platforms, very few papers report a full system implementation and those reported are laboratory prototypes. Four radar prototypes implementing Multitones signals were reviewed and compared: PANDORA [10] which is the first experimental OFDM radar, an RCS measuring system [11], a dual use SAR imaging and telecommunications system [6] and a Software Defined Radio platform IDROMel [12].

A few design rules can be drawn from these architectures. First, if the AD/DA converters' instantaneous bandwidth and/or sampling frequency are not sufficient for direct synthesis or direct sampling, a super-heterodyne structure is required. The radar prototypes display submetric spatial resolution and thus digitizers sampling frequencies are at least 1 GS/s. However sampling schemes are diverse: sub-Nyquist, bandpass or direct. Finally, the frequency tuning ranges are at least 1 GHz wide. The design of the architecture should be kept simple, with as little components as possible, one or two down-conversions at most. Unlike Chirp signal, stretch processing isn't applicable to Multitones thus whichever waveform is used, it should be fully digitized.

Reconfigurable radar technology is still in its early stage. The reconfiguration is limited in terms of the number of carriers, the step size, the bandwidth, or its hardware architecture has to be split into several sub-bands. These features are usually at the cost of increased hardware complexity or increased interferences in the receiver.

III. CONCEPTION OF SOFTWARE-DEFINED RADAR

This section is a description of an approach that can be used for an unbiased study of radar waveforms to the implementation of the prototype examined in this study.

A. Design approach for an unbiased experimental study

In order to unbiasedly compare different waveforms, it is essential that waveform-independent criteria are used. Further, to evaluate the performances without bias, the simulated processes and the experimental test bench should be identical. The maximum detection range and pulse compression in range profile can be used as a first step to evaluate radar waveform performances.

To compare the different waveforms, it is not sufficient to simply examine simulation results; and thus this comparison should be experimentally validated. It is therefore necessary to develop a software defined radar prototype that can test the waveforms under study without any bias. The novel approach is to compare the studied waveforms on the same platform to remove any bias. In this paper, simulations and measurements are designed to provide the basis for an unbiased study of the radar waveforms.

It should be noted that the radar prototype should be designed prior to the simulations, this way the characteristics of the prototype can then be fed to the simulator for a subsequent and direct comparison between simulated and experimental results.

B. Experimental Design

1) Design of RF system

A few constraints were established for the test bench design. The first step was to optimize the instantaneous bandwidth to maximize the radar spatial resolution. Hence, the bandwidth should be greater than 500 MHz to perform as well as state of the art radar prototypes [6][10][11]. The radar should support any type of waveform with no changes to the RF frontend. These two requirements ensure an unbiased study of various waveforms on the same prototype. Also a reference channel is implemented to compensate for some of the circuit transfer function. This constraint is a special feature that is not normally implemented in operational radar systems but does allow refreshing the matched filter dynamically to compensate for any fluctuations in transfer function especially with power amplifiers.

Due to spatial constraints on the experimental grounds, a maximum of 50 m in slant range is achievable. Consequently, the architecture must be bi-static and emit in continuous wave to allow for pulse compression gain greater than 20 dB.

Two architectures are proposed as candidates for the implementation: frequency-interleaved, parallel. The frequency-interleaved architecture is inspired from the prototype in [11]. It is investigated because it reduces the number of components and the number of ADC channels. The parallel architecture is derived from the frequency interleaved architecture. Although more components are required, it has a potential for more versatile usage.

a) Parallel architecture

A synoptic of the parallel architecture is shown in Figure I. The signal is directly synthesized in intermediate frequencies (IF) ranging from 1 to 2 GHz and a low pass filter removes the mirror image. The IF signal is up-converted in radio frequencies (RF) ranging from 9.9 to 10.9 GHz by F_{LO1} = 8.9 GHz, and a band pass filter removes the mirror image. For short range applications, the signal can be amplified by a low noise amplifier; and for longer ranges, a power amplifier can be used. At the output of the amplifier stage, a 20dB directional coupler splits the signal: the coupled output feeds the signal to the reference channel and the direct path is connected to the transmitter antenna feed. The backscattered signal is received by the second antenna which is connected to the test channel. The received signal travels through a low noise amplifier and a band pass filter removes the mirror image before down-conversion by F_{LO1} = 8.9 GHz. The signal in the reference channel is attenuated and down-converted by $F_{LO2} = F_{LO1}$ = 8.9 GHz. In both the reference and the test channels, the signals are band pass filtered to avoid aliasing and are then amplified prior to digitization.

b) Frequency-interleaved architecture

The radar operates in continuous wave mode; thus the spectra of any signal is discrete and the frequency step Δf (e.g. 2 MHz) is the inverse of the signal period T (e.g. 500 ns). This property is exploited to design the frequency-interleaved architecture.

Paichard [11] provides a conceptual framework for the development of the frequency-interleaved architecture used in this study. Compared to the parallel architecture, the reference channel down-conversion-frequency is F_{LO2} = 9 GHz = $F_{LO1}+\Delta f/2$. Since the frequencies of the test channel and reference channel are not overlapping, they can be added using a power combiner, thus both signals are merged together, and the frequency step of the resulting signal is $\Delta f/2$ = 1 MHz. This architecture presents the advantage of digitizing the reference and test signals on the same ADC, thus reducing by half the number of required ADC channels as well as reducing the number of components.

2) Design of the Signal processing algorithms

The algorithms were designed to process signals impartially to allow for an unbiased comparison. Radar systems use pulse compression in order to detect targets; the optimum match filtering process in white Gaussian Noise was chosen for implementation.

Two algorithms were used :

- The first algorithm employed radix-2 FFT and is suitable only for the parallel architecture.
- The second algorithm used DFT due to constraints on data extraction for frequency-interleaved signals.

In both cases, the only variable in the algorithms is the input vector size, no other reconfiguration is necessary. Section 3 estimates the required processing power for each architecture; considering the Neptune VXS 2 [13] ADC will be implemented for digitization at 2GS/s.

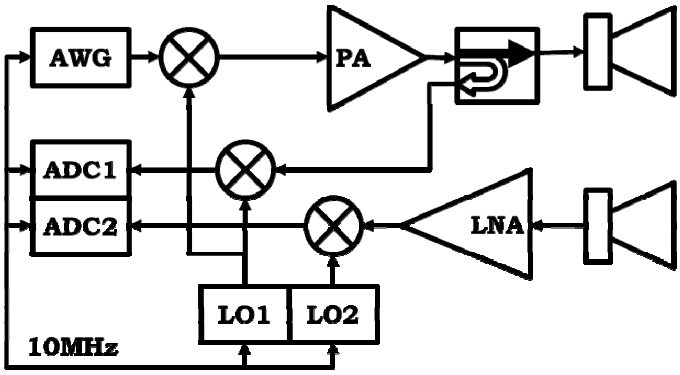

Figure I: synoptic of parallel architecture

a) Radix-2 FFT algorithm for parallel architecture

Figure II describes the Radix-2 FFT algorithm. Two input signals are necessary: the reference signal and the test signal. The reference signal is used to generate the matched filter. It can either be a digital replica or a measured replica of the generated signal. The replica can either be fixed or refreshed at a given frequency.

Since the test signal delay is unknown *a priori*, a sliding window that is three times the signal period is implemented for the test channel. This guarantees that whatever the signal returns delays are, a complete impulse response is generated without losses on the edges of the pulse compression. Hence, this algorithm is suitable for either the parallel or the time-interleaved architectures.

Both vectors have unit sizes equal to M (e.g. 1000) which is the signal period T (e.g. 500ns) times the sampling frequency (2GS/s). For faster processing, radix-2 FFT is used, thus the digitized vector length $3M$ for the test channel and M for the reference channel are zero-padded **ZP** up to the next power of 2 greater than $(4M-1)$. (4M-1) is the size of the cross-correlation between $3M$ and M. The radar system only generates the real part of the signal. The complex values of the signal must therefore be reconstructed using a Hilbert transform $\hat{\mathbf{H}}$.

The signals are digitally down-converted to baseband **BB**, then, a window function **w(n)**, such as Rectangle or Hamming, is applied over the pulse length M on the reference. The apodization by Hamming window limits the effect of inter-symbol interference (ISI) for telecommunication signals and increases the contrast of the impulse response at the cost of a 38 % widening of the main lobe at 3 dB. A radix-2 **FFT** is applied on both test and reference signals to move to frequency domain. The complex conjugate **()*** of the reference signal is multiplied element by element to the test signal. This operation is equivalent to a cross-correlation in time domain. Then, to obtain the impulse response in time domain, a radix-2 **IFFT** is applied. The complete pulse compression ranges from $M/2$ to $(3M/2-1)$, giving a zero delayed response centred within that window.

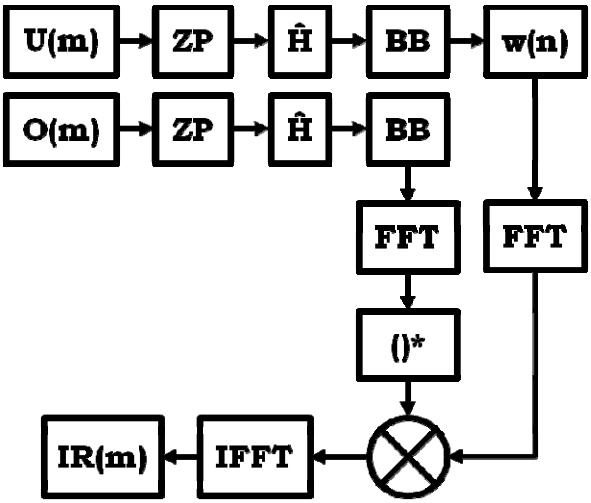

Figure II: Radix-2 FFT algorithm

b) DFT algorithm for frequency-interleaved architecture

The frequency-interleaved architecture intertwines both reference and test signals into a common signal. The reference signal is shifted in frequency by half the inverse of the pulse repetition period $1/(2T) = \Delta f/2 = 1$ *MHz* compared to the test signal. The principle of the pulse compression algorithm for frequency-interleaved signals is described in Figure III.

Since the frequency step of the signal is now $\Delta f/2$. The signal period is doubled. At least $2M$ (e.g. 2000) samples are necessary for the extraction of both signals. A Hilbert transform $\hat{\mathbf{H}}$ is applied to the signal. The signal is then down-converted in baseband **BB**. A **DFT** is used to move to frequency domain to extract the reference and test signals before realizing the pulse compression. Odd samples go to the test channel vector and even samples go to the reference channel.

The reference signal on M samples is then switched back to time domain using an **IDFT**. This operation enables the final down-conversion **BB** to compensate for the slight phase modulation resulting from the frequency shift $\Delta f/2$. A window **w(n)** can be applied in a time domain.

The reference signal is returned to frequency domain with a **DFT**. Its complex conjugate **()*** is multiplied element by element to the test signal. This realizes the equivalent of a time domain cross-correlation. Finally an **IDFT** is applied to obtain the pulse compression.

C. Initial considerations for experimental implementation

In order to quantify the required processing power, the characteristics of the Neptune VXS 2 [13] ADC that will be implemented in the radar will be used for the estimations. The ADC Neptune VXS 2 encodes the samples on 10 bits, meaning that the data is encoded on 2 bytes. Thus the data flux is 4 GB/s per channel at 2 GS/s when digitizing continuously.

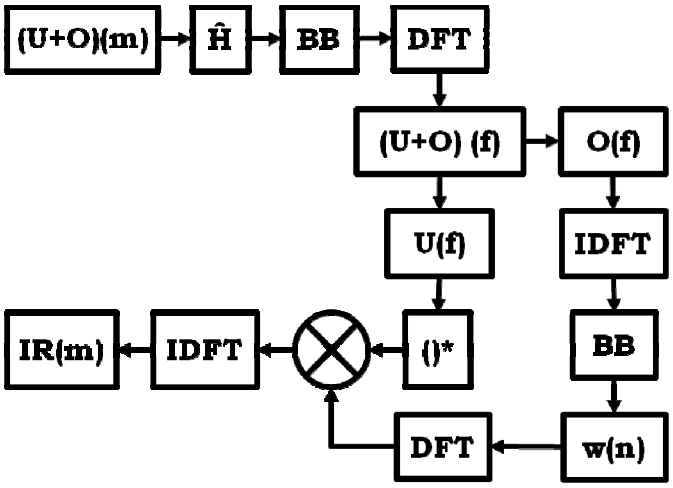

Figure III: DFT algorithm

The comparison in processing power is based on the number of real multiply accumulate operation per seconds (MACS) required to obtain pulse compression in real-time. The required processing powers for the frequency-interleaved, parallel and time-interleaved architectures are respectively given in equations (1) and (2) below. Results are shown in Figure IV.

$$5M(12nM + 1) \cdot T_{orth}{}^{-1} \quad (1)$$

$$\left(6M + 35 \cdot 2^{Y} n(Y + 1)\right) \cdot T_{orth}{}^{-1} \quad (2)$$

Where n is the number of channels, M *is the* vector length and Y is an integer so that $4M \leqslant 2^{Y}$

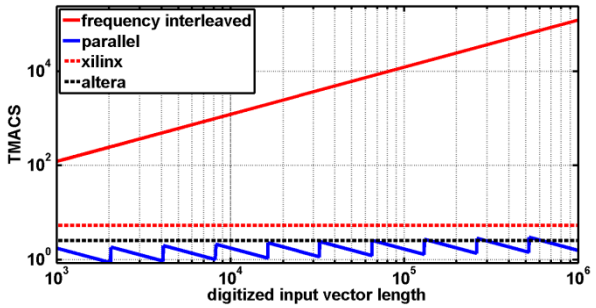

Figure IV: required processing power for the proposed radar architectures in TMACS (10^{12}MACS) wrt to input vector length – considering a sampling frequency of 2GS/s, a word length of 10bits

Figure IV illustrates that the processing for frequency-interleaved architecture is intractable and therefore dismissed for implementation. The processing power for the other architecture is in the TMACS (10^{12}MACS) region but within reach for the announced capabilities of the newest generation of FPGAs. The Altera Stratix V [14] performs up to 2.5 TMACS and Xilinx Virtex 7 [15] performs up to 5.314 TMACS. Although the algorithm for any vector length still has to be implemented on FPGA, real-time signal processing with two ADC channels at 2 GS/s and a resolution of 10 bits is feasible.

Even if the processing power is within reach, decimation strategies and other pre-processing schemes should be

investigated to reduce the required MACS and data throughput for storage. If the radar uses pulse bursts rather than continuous wave emission, these requirements would be reduced proportionally with the pulse repetition period at a given pulse length.

IV. EXPERIMENTAL SETUP OF THE SOFTWARE DEFINED RADAR PROTOTYPE IMPLEMENTATION

As illustrated in Figure V, the implementation of the radar prototype is detailed [16]. The radar has 800 MHz instantaneous bandwidth per channel, emits in X-band between 10 GHz and 11.6 GHz. It has 1.6 GHz agility and has AD/DA converter resolution of either 8 or 10 bits. This prototype supports any kind of waveforms for an unbiased analysis. The waveform agility is digitally controlled and no hardware modification is required.

Table I compares the characteristics of the proposed prototype to those of the platforms as found in [6][10][11][12]. This software defined radar prototype is comparable in performances with state of the art platforms. This prototype digitizes 800 MHz on a single ADC rather than 8 channels as proposed in [10], 800 MHz on 2 channels in [11] or 500 MHz on a single channel in [6]. It supports any waveforms unlike [11] that can only process OFDM in burst mode. In [12], the architecture's agility is 7 GHz with 20 MHz bandwidth where this prototype gives 800 MHz instantaneous bandwidth and 1.6GHz agility.

In Figure VI, the trihedral reflector is at the centre of the scene and distant of 27.75 m. It has a radar cross-section of 30 dBsqm thus giving a contrast of 59 dB between the reflector and the clutter. The trihedral reflector allows for reproducible experiments since it is a static target and that the signals will be measured consecutively. Further details about the experimental setup can be found in [16]. The measurements are recorded on a hard disk drive and the data is processed **offline** using MATLAB.

The selection of appropriate radar architecture (frontend+algorithm) and the design of reproducible experiment constitute the basis to follow the approach for an unbiased study.

In Figure VI, the trihedral reflector is at the centre of the scene and distant of 27.75 m. It has a radar cross-section of 30 dBsqm thus giving a contrast of 59 dB between the reflector and the clutter. The trihedral reflector allows for reproducible experiments since it is a static target and that the signals will be measured consecutively. Further details about the experimental setup can be found in [16].

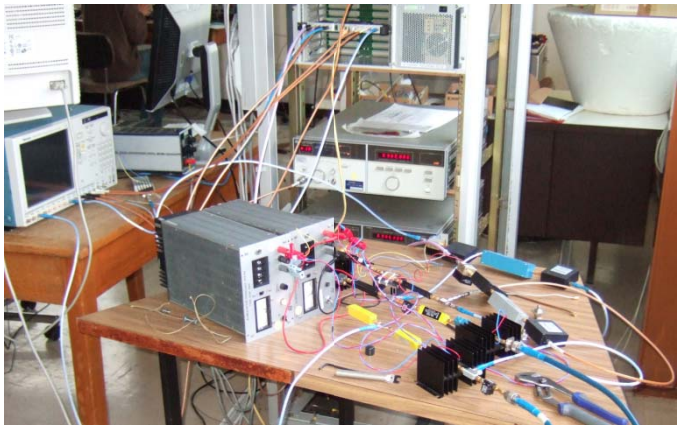

Figure V: prototype

Table I: comparison of the the prototype to the RF platforms from the literature review

platform	PANDORA [10]	RCS meas. syst. [11]	SAR imaging and telecom. [6]	IDROMel [12]	This work
Instantaneous bandwidth	776 MHz	800 MHz	500 MHz	20 MHz	800 MHz
Range resolution	0.19 m	N/A	0.3 m	N/A	0.1875 m
Tested range	N/A	10 m	1.5 to 5 m	N/A	60 m
Sampling scheme	Shannon	Sub-Nyquist + Bandpass	Shannon	Shannon	Bandpass
Sampling frequency	N/A	1.35 GS/s	1 GS/s	N/A	2 GS/s
Frequency Tuning Range	8 to 12 GHz	10 to 11.6 GHz	7 to 8 GHz	0.4 to 7.5 GHz	10 to 11.6GHz
Architecture	Super-heterodyne + stretch processing	Super-heterodyne + frequency-interleaving	Super-heterodyne	Super-heterodyne + 4x4 MIMO + I/Q channels	Super-heterodyne
Supported waveforms	Stepped Multitones, multiband FMCW	Multitones	Multitones	UMTS, GSM, IEEE.802.11/16	any
Pulse width	3.125 ms per step	100 to 200 ns	128 to 512 ns	Dependent on standard	500 ns up to 1 ms

Figure VI: experimental setup

The selection of appropriate radar architecture (frontend+algorithm), the design of reproducible experiment constitute the basis to follow the approach for an unbiased study.

V. Experimental results: Comparison of radar waveforms

A. Studied Radar waveforms

The radar emits in continuous wave and the waveforms will cover the bandwidths (B) of 1 MHz, 10 MHz, 150 MHz and 800 MHz, and pulse repetition period (T) of 500 ns, 5 µs, 50 µs, 500 µs and 1 ms. Each bandwidth value will be tested with every values of T (the exception being BxT products lower than 75). The IF sampling frequency is 2 GS/s and the IF frequency range is centered on 1.5 GHz, the signal instantaneous bandwidth varies from 1 MHz to 800 MHz.

The studied signals are the P3 phase-coded [2] Multitones and the linear Chirp. The latter is a reference in the radar community and thus is used to evaluate the performances of Multitones.

The waveforms' continuous time equations are shown below in equations 3 and 4 (for Chirp and Multitones, respectively).

$$upC(t) = real\left(exp\left(i2\pi\left(f_0 + \frac{B}{2T}t\right)t\right)\right) \quad (3)$$

$$MT(t) = real\left(\sum_{n=0}^{N-1} exp\left(i2\pi(\delta f(n_0+n)t + \phi_n)\right)\right) \quad (4)$$

where $\phi_n = N^{-1}\pi(n-1)^2$ is the P3 phase code and t belongs to $[0;T[$, T is the pulse width and the orthogonal period for Multitones, $B = N\delta f$ are the signals' bandwidth, N is an integer and the number of tones, $\delta f = T^{-1}$ is the Multitones' frequency step. $f_0 = n_0\delta f$ are the signals's starting frequencies. Keeping the orthogonality for Multitones will yield the best result for impulse response. The discrete time equations of both signals Chirp (3) and Multitones (4) are defined in equations (5) and (6) respectively for a sampling frequency F_S and a sampling time t_S. First, a condition is set $T = Mt_S$ and M is an integer.

$$upC(m) = real\left(exp\left(i2\pi\left(n_0 + N\frac{m}{2M}\right)\frac{m}{M}\right)\right) \quad (5)$$

$$MT(m) = real\left(\sum_{n=0}^{N-1} exp\left(i2\pi\left((n1_0+n)\frac{m}{M} + \phi_n\right)\right)\right) \quad (6)$$

m is the sample number and belongs to $[0;M[$.

It should be noted that Multitones need to respect constraints at the generation and digitization to avoid intermodulation interference. So Chirp can achieve better linearity with little constraints.

B. Simulations and experimental results on pulse compression

Comparing theory and simulation, the results may differ from the expected value and at first glance, variations in the results might appear inconsistent with theory (Table II). However it should be noted that sampling the IF signal produces a regular spatial speck proportional to the IF sampling frequency. At 2 GS/s, this sampling speck is equal to 0.075 m. The 3 dB main-lobe width and the sidelobes' positions are within 10 % of the expected value for all configurations, except when the speck is large compared to the resolution as for 800 MHz where the error is within 38 %.

The simulation of pulse compression either with a rectangular or a Hamming window yielded results that are coherent with the theoretical values for main-lobe width, sidelobes' positions and amplitudes. The Chirp and Multitones offer the same performances regarding detection capabilities as shown in Table II and the sidelobe's amplitude is -13.27 dB for all cases.

Table II: simulated results at 2 GS/s for pulse compression with rectangular window for Chirp and P3 Phase-Coded Multitones

Bandwidth	1 MHz	10 MHz	150 MHz	800 MHz
Mainlobe 3dB-width	133 m	13.3 m	0.9 m	0.225 m
Sidelobes' positions DSL1/DSL2	±214.8 m	±21.4 m	±1.425 m	±0.3 m

Figures VII and VIII depict the pulse compression for Chirp and Multitones on a trihedral reflector 5.2 m further in slant range than shown in Figure V. The distance can be measured at 5.121 m which is coherent with the value measured physically. The error of 0.08 m is acceptable considering the range resolution 0.1875 m and the sampling speck 0.075 m.

The relative error on 3 dB mainlobe width, sidelobes' positions and difference in sidelobes' amplitudes between measurements and simulations is shown in Table III. The large errors for 3 dB mainlobe width and sidelobes positions at 800 MHz are caused by sample speck and perturbations induced by standing wave ratios in the circuit and clutter. Otherwise, the signals from 1 MHz to 150 MHz are within 3.1 % of the expected values, for 3 dB mainlobe width and sidelobe positions, and the difference in sidelobes amplitudes are lower than 0.3 dB. Both waveforms Chirp and Multitones are equivalent on pulse compression in the range profile.

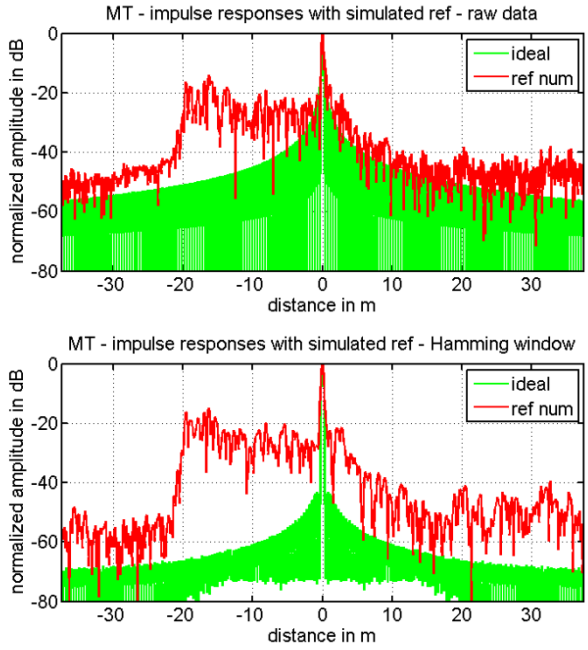

Figure VII: measured pulse compression on trihedal reflector - distance 5.2 m - Newman Phase-Coded Multitones (MT) with 800 MHz bandwidth and 5 µs pulse repetition period

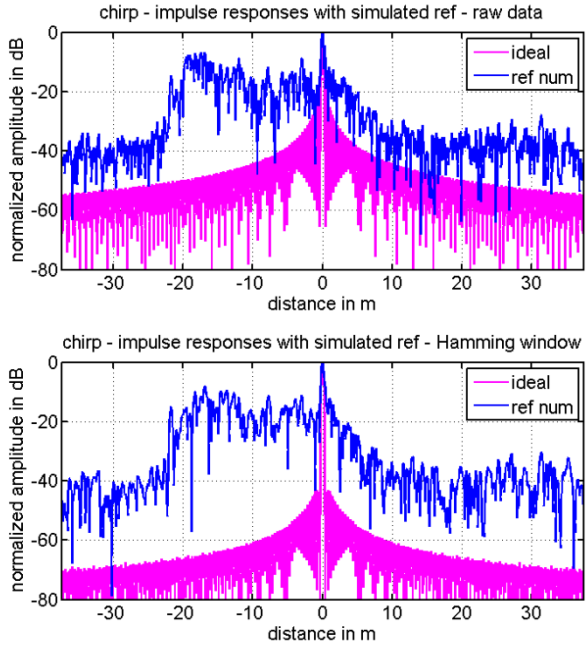

Figure VIII: measured pulse compression on trihedal reflector - distance 5.2 m – P3 Phase-Coded Multitones (MT) with 800 MHz bandwidth and 5 µs pulse repetition period

Table III:relative error on 3 dB mainlobe width, sidelobes' positions and difference in sidelobes' amplitudes between measurements and simulations

Bandwidth	1 MHz	10 MHz	150 MHz	800 MHz
3 dB Mainlobe width	<1.9 %	<1.8 %	<2.3 %	<37 %
Sidelobe amplitudes	<0.3 dB	<0.3 dB	<0.3 dB	[-7;3 dB]
Sidelobe positions	<0.7 %	<1.7 %	< 3.1 %	<67 %

C. Simulations and experimental results on detection range

The difference in detection range capabilities between both waveforms are evaluated based on the Peak-to-Mean Envelope Power Ratio (PMEPR) and the power efficiency (η). The PMEPR results range from 3.01 to 3.2 dB for Chirp and 5.44 to 5.65 dB. As for power efficiency, simulations show a relative error of 2% in favor of Multitones which is negligible. From measurements, the PMEPR results range from 3.2 to 4.22 dB for Chirp and 5 to 6.2 dB for Multitones. The discrepancies are larger in wideband than in narrowband caused by standing waves in the test bench. Concerning power efficiency, the results match simulations.

Using the monostatic radar equation, the results show that using Chirp yields an extended detection range of 13 to 17 % in simulations and 5 to 19% compared to using P3 phase-coded Multitones. The discrepancies are larger in wideband than in narrowband caused by standing waves in the test bench. This shows that Chirp on average yields an extension of 15 % in detection range compared to Multitones.

VI. CONCLUSION

This paper proposed and tested an approach for an unbiased study of radar waveforms' performances. A test-bench was designed and implemented to allow a direct unbiased comparison of simulated and experimental results. The architecture was implemented and has performances comparable to the state of the art in software defined radar prototypes [6][10][11][12]. All signal processing was performed offline using Matlab.

Based on simulations and experimental validations, it was shown that Chirp and P3 phase-coded Multitones have the same performances in range profile detection. However Chirp provides an extra 15 % in detection range compared to Multitones. The measurements (up to 150 MHz bandwidth) matched the simulation results, thereby validating the approach for the implementation of the experimental test-bench for an unbiased study of radar waveforms.

While Multitones incorporates the telecommunication function to the radar, the trade-off of at least 15% loss in detection range (for modulation with the same PMEPR reduction capability as P3 codes). Even though Multitones are not superior to other waveforms for all applications (outside of telecommunications), they outperform other waveforms in a multifunction scenario (such as telecommunications combined with radar applications). As such, Multitones can be thought of as the decathlete of waveforms – not be the best in any individual discipline but the best overall. Therefore Multitones is an optimal waveform for overall performance.

Furthermore new processing capabilities have recently emerged using Multitones (such as Doppler processing while using agility [8] and solving Doppler ambiguity [9] which cannot be achieved with Chirp). For long range applications, Chirp is likely to remain the waveform of choice. Multitones is likely to be the waveform of choice for short to mid-range applications – and is very likely to succeed to Chirp in the future.

The outcome of this research showed that the required processing power is greater than what can be provided by the latest FPGA chipsets using state of the art ADC. Based on the proposed equipment and architectures, the required processing power for the parallel architecture is within reach in processing power with the latest Virtex 7 [15]. The algorithm implementation on FPGA remains and it is likely that real-time processing will require several chipsets, parallel processing of the quantized signal, some pre-processing schemes and/or decimation to reach this goal. Other technological bottlenecks such as bus communication speed and writing speed for storage will hinder real-time applications. So for now UWB software defined prototypes will have to process the data offline and perform measurements in bursts and store rather than continuous operation.

VII. PERSPECTIVES FOR FUTURE RESEARCH

The architecture examined in this research can be further improved by time-interleaving the test and reference channel; thus reducing the number of components and the required processing power while keeping versatility. In the time-interleaved architecture switches would shunt the antennas to measure a reference, hence interrupting detection. Furthermore there are added constraints on synchronization for switching operations and stability to limit the frequency of the calibration cycle. The development of new architectures (RF system + algorithms) holds the promise of continuing to reduce the processing power requirement and data throughputs, which are the primary bottlenecks towards real-time processing.

The algorithm proposed in this work is only the first step for the detection, and current trends indicate that real-time algorithms will be implemented on a single-chip. With ever growing data throughputs, the intra-chip interconnections are becoming more and more of an issue that needs to be addressed.

Using multitones for radar applications means observing moving targets, the Doppler will affect the orthogonality and thus performances may vary depending on the phase coding. Hence a trade-off between telecommunications and radar functions will need to be found. The performances of various phase codes need to be investigated. Multifunction scenarios means signal diversity and notched spectra hence performances in such configurations will need to be addressed.

REFERENCES

[1] J. Terry, J. Heiskala, *OFDM Wireless LANs: A Theoretical and Practical Guide*, 2002, Sams Publishing

[2] Radar signals. N. Levanon, E. Mozeson, 2004, editor John Wiley & Sons

[3] Simulated Imaging Performance of UWB SAR Based on OFDM. D.S Garmatyuk, 2006. Proceedings of IEEE International Conference on Ultra-Wideband. pp. 237-242.

[4] Waveshaping of multicarrier signal for data transmission over wireless channels. H. Nikookar, and R. Prasad, 1997, IEEE 6th International Conference on Universal Personal Communications Record Conference Record, pp. 173-177.

[5] Train of diverse multifrequency radar pulses. N. Levanon, 2001. Proceedings of IEEE Radar Conference, pp. 93-98.

[6] Radar and data communication fusion with UWB-OFDM software-defined system. Garmatyuk, D. et Kauffman, K. 2009. Proc. IEEE International Conference on Ultra-Wideband ICUWB 2009. pp. 454-458.

[7] Improvement in target detection performance of pulse coded Doppler radar based on multicarrier modulation with fast Fourier transform (FFT). N. N. S. S. R. K. Prasad, V. Shameem, U. B. Desai, S. N. Merchant, 2004, IEE Proceedings -Radar, Sonar and Navigation, Vol. 151, pp. 11-17.

[8] OFDM waveforms for frequency agility and opportunities for Doppler processing in radar. G. Lellouch, P. Tran, R. Pribic and P. van Genderen, 2008, RADAR '08 - Proceedings of IEEE Radar Conference, pp. 1-6

[9] Solving Doppler ambiguity by Doppler sensitive pulse compression using multi-carrier waveform. R.F. Tigrek, W.J.A. de Heij, P. van Genderen, 2008, EuRAD 2008 - Proceedings of European Radar Conference, pp. 72-75.

[10] Pandora multifrequency FMCW/SFCW radar. M. Jankiraman, B.J. Wessels, P. Van Genderen, Proceedings of the IEEE 2000 International Radar Conference, pp. 750-757

[11] Paichard, Y. Microwave Camera for Multi-Dimensional Analysis of the RCS of Time-Varying targets. University of Paris 11. 2007.

[12] **www.openairinterface.org.** Open Air Interface - IDROMel. *Open Air Interface - IDROMel.*

[13] www.tekmicro.com. tekmicro.

[14] www.altera.com, Stratix V

[15] www.xilinx.com, Virtex 7

[16] Case study analysis of linear Chirp and multi-tones radar signals through simulations and measurement with HYCAM-Research Test Bench, J. Le Kernec, P. Dreuillet, G. Bobillot, J.C. Castelli, P. Garda, O. Romain, J. Denoulet, 2009, Radar Conference - Surveillance for a Safer World, pp 1-5